論文

직교이방성판의 좌굴강도를 구하기 위한 근사식의 개발

정재호*+, 윤순종*, 유성근**

Approximate Solution for Finding the Buckling Strength of Orthotropic Rectangular Plates

J. H. Jung*+, S. J. Yoon*, S. K. You**

ABSTRACT

In this study, the analytical investigation of orthotropic rectangular plate is presented. The loaded edges are assumed to be simply supported and the unloaded edges could have elastically restrained boundary conditions including the extreme boundary condition such as simple, fixed, and free. Using the closed-form solutions, the buckling analyses of orthotropic plate with arbitrary boundary conditions are performed. Based on the data obtained by conducting numerical analysis, the simplified form of equation for finding the buckling coefficient of plate with elastically restrained boundary conditions at the unloaded edges is suggested as a function of aspect ratio, elastic restraint, and material properties of the plate. The results of buckling analyses by closed-form solution and simplified form of solution are compared for various orthotropic material properties. It is confirmed that the difference of results is less than 1.5%.

초 록

본 연구는 면내 선형분포하중이 작용하는 직교이방성판의 좌굴거동에 관한 것으로서, 하중이 재하된 두 변은 단순지지되어 있으며 하중이 재하되지 않은 두 변은 회전에 대해 탄성구속된 경계조건을 포함하여 다양한 경계조건을 갖는 직교이방성판의 좌굴해석식을 정밀해법을 사용하여 유도하였다. 좌굴해석 수행 결과를 사용하여 하중이 재하되지 않은 두 변이 특정 경계조건인 경우를 포함하여 회전에 대해 탄성구속된 판의 좌굴해석을 위한 근사식을 판의 형상비와 탄성구속 정도를 나타내는 계수 및 재료의 성질의 함수로 제시하였다. 제시된 근사식을 사용할 경우 재료의 성질과 판의 형상비 및 하중이 재하되지 않은 변의 탄성구속정도를 알면 단순계산으로 직교이방성판의 좌굴해석을 수행할 수 있도록 하였다. 여러 가지 직교이방성 재료에 대해 근사식에 의한 해석결과와 정밀해법에 의한 해석결과를 비교한 결과 1.5% 미만의 차를 나타냈었다.

Key Works : 직교이방성판(Orthotropic plate), 좌굴계수(Buckling coefficient), 탄성구속(Elastic restraint), 근사식(Approximate solution)

1. Introduction

Fiber reinforced plastics (FRP), limitedly used to aerospace structures, are gaining broad acceptance in civil engineering applications gradually. Growing maintenance demand and durability problems in existing infrastructures made of

*+ 홍익대학교 대학원 토목공학과, 교신저자(E-mail:hih-jung@hanmail.net)
* 홍익대학교 공과대학 토목공학과
*** BBM Korea

conventional material such as concrete and steel have led researchers to develop FRP structural members.

In many manufacturing techniques of FRP structural shapes, the pultrusion process is becoming a popular one for producing relatively low-cost FRP structural members in civil engineering fields. The pultreded FRP structural shapes are usually composed of thin-walled plate elements. In the design of such a structural member, the local buckling can be one of the major failure modes since the material has low stiffness, which is prone to deflect, and it remains linearly elastic for large deflections and strains, unlike the conventional construction materials that yield (structural steel) or crack (concrete) for moderate strains.

In the local buckling analysis of thin-walled structural members, it was assumed that the plate junctions remain straight and the angles between plates at the junction remain constant during local buckling. Therefore, the local bucking indicates the buckling of plate components and the study on the behavior of plate buckling can give a fundamental knowledge of local buckling problem.

The mechanical properties of pultruded fiber reinforced plastics were approximated as orthotropic due to the reinforcing nature of fibers (i.e., unidirectional) in the early years of 1990th and those were obtained by performing coupon test. In recent years, it was also accepted that pultruded sections can be simulated as laminated composites and Davalos et al. (1996) showed that the mechanical properties and stiffness of plate component can be predicted by using the micromechanics formulae and classical lamination theory [1].

In this study, brief review of general solution for finding the buckling strength of isolated plate component of pultruded structural members is presented. The isolated plate component is approximated as a specially orthotropic (transversely isotropic) plate subjected to linearly varying in-plane forces and its loaded edges are assumed to be simply supported considering the practical behavior of structural members. The unloaded edge can be not only the extreme boundary condition such as simple, fixed, and free, but also the rotationally restrained if the unloaded edge is the common junction of plate components.

Conducting the buckling analyses with various material properties and numerical analysis, the simplified form of equation is suggested for orthotropic plate buckling problem. The results obtained by proposed simplified form of equation are compared with those of closed-form solution.

2. Previous Work

The instability problem of isolated orthotropic plate have been well documented by many engineers and scientists. Wittrick (1952) investigated the correlation between some stability problems for orthotropic and isotropic plates under bi-axial and uni-axial direct stresses [2]. Lekhnitskii (1968) [3] published the closed-form solutions for buckling of orthotropic plate with various boundary conditions. Those solutions of orthotropic plate buckling under uniform compression were applied to derive the local buckling equation of orthotropic thin-walled compression members by Lee (1978, 1979) [4, 5], Yoon (1993) [6], Chae (1994) [7], etc.

Shih (1994) [8] developed a general analytical solution pertaining to the buckling behavior of transversely isotropic plates subjected to linearly varying in-plane stresses along the loaded edges. In his work, the solutions for local buckling problem of orthotropic flexural members were presented by using the buckling equation of orthotropic plates.

Webber, et al. (1985) [9], Bank (1996) [10], and Yoon et al. (1999) [11] were derived the buckling equation of orthotropic plate with restrained and free edges under uniform compression. Yoon, et al. (2000) [12] published the results of buckling analysis of restrained orthotropic plate under linearly distributed in-plane forces by using the Rayleigh-Ritz method.

Since the buckling equations obtained in the previous works were the transcendental forms, the equations obtained are very complex and too difficult to use in practical design. Unlike the conventional material such as a structural steel, FRP has complex material properties and its mechanical properties vary depending upon the reinforcing fiber and its containment. Therefore, it is necessary to develop the simplified form of equation convenient for the engineers in practice and to establish the rational design criteria of the member.

3. Closed-form Solution

Consider an isolated homogeneous orthotropic plate subjected to linearly distributed in-plane forces as shown in Fig. 1. The loaded edges are assumed to be simply supported and the unloaded edges can be arbitrary boundary conditions including elastically restrained boundary. The length and width of plate are a and b, respectively, and t is the thickness of plate. E_x and E_y are the Youngs moduli of plate in longitudinal and transverse directions, respectively, and those can be obtained by coupon test and predicted by using

the micromechanics formulae and the classical lamination theory [1]. $\xi (=x/a)$ and $\eta (=y/b)$ are the nondimensionalized Cartesian coordinates.

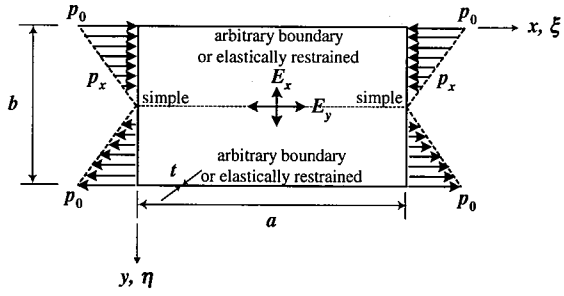

Fig. 1 Orthotropic rectangular plate.

The applied linearly distributed loads can be written in terms of constant c which represents the distribution of loads as given by Eq. (1). When c is zero uniformly distributed loads are applied, and when c equals to 2.0 triangularly distributed compressive and tensile loads are applied.

$$p_x = p_0(1 - c\eta) \tag{1}$$

When the unloaded edges are elastically restrained, the coefficient of elastic restraint ε can be expressed as follows:

$$\varepsilon = \frac{\zeta b}{D_y} \tag{2}$$

In Eq. (2), ζ is the restraining moment along the rotationally restrained edge per unit length per unit rotation. When ε is equal to zero it stands for a simple support, and when ε goes to infinity it corresponds to a fixed support.

3.1 Basic equations

For the orthotropic plate as shown in Fig. 1, the governing differential equation for buckling based on the small deflection theory can be stated as Eq. (3) by using the dimensionless parameters.

$$\lambda_1^4 s^4 \frac{\partial^4 w}{\partial \xi^4} + 2\lambda_2^2 s^2 \frac{\partial^4 w}{\partial \xi^2 \partial \eta^2} + \frac{\partial^4 w}{\partial \eta^4} + \pi^2 k(1 - c\eta)\lambda_1^2 s^2 \frac{\partial^2 w}{\partial \xi^2} = 0 \tag{3}$$

In Eq. (3), the letter w indicates the out of plane deflection of plate and s is the ratio of width to length of plate ($= b/a$). The dimensionless buckling coefficient k and dimensionless parameters λ_1 and λ_2 are defined as follows:

$$k = \frac{p_0 b^2}{\pi^2 \sqrt{D_x D_y}} \quad \lambda_1 = \left(\frac{D_x}{D_y}\right)^{1/4} \quad \lambda_2 = \left(\frac{\nu_{yx} D_x + 2D_{xy}}{D_y}\right)^{1/2} \text{(4 a,b,c)}$$

where,

$$D_x = \frac{E_x t^3}{12(1 - \nu_{xy}\nu_{yx})}, \quad D_y = \frac{E_y t^3}{12(1 - \nu_{xy}\nu_{yx})} \tag{5 a,b}$$

$$D_{xy} = \frac{G_{xy} t^3}{12}, \quad \nu_{xy} E_y = \nu_{yx} E_x \tag{5 c,d}$$

The general solution of Eq. (3) can be obtained as Eq. (6) by assuming the deflection function in the transverse direction as the power series functions [8].

$$w = \left\{A_0\left(\sum_{n=0}^{\infty} B_{n,0}\eta^n\right) + A_1\left(\sum_{n=0}^{\infty} B_{n,1}\eta^n\right) + A_2\left(\sum_{n=0}^{\infty} B_{n,2}\eta^n\right) + A_3\left(\sum_{n=0}^{\infty} B_{n,3}\eta^n\right)\right\} \sin m\pi\xi \tag{6}$$

In Eq. (6), m is the number of half-sine waves along the ξ-axis. A_i with i = 0, 1, 2, and 3 are constants that must be determined from the boundary conditions along the unloaded edges, η = 0, 1, and the $B_{n,i}$ with i = 0, 1, 2, and 3, are given in Appendix.

3.2 Determinantal form of Equations

As previously mentioned, A_i with i = 0, 1, 2, and 3 are constants that must be determined from the boundary conditions along the unloaded edges, η = 0, 1. Conditions of various boundaries are presented in Table 1.

Upon substituting Eq. (6) into the boundary conditions as indicated boundaries, two of each boundary, four distinct simultaneous linear homogeneous equations for A_i are obtained, and except for the case of restrained boundary conditions the size of simultaneous equations are reduced to two by two. Table 2 shows the characteristic function of plate buckling for various boundary conditions along the unloaded edges.

In Table 2, ε_1 and ε_2 are the coefficient of elastic restraint at the unloaded edges, η = 0, 1, respectively. Equating the characteristic equation in Table 2 to zero, the buckling coefficient defined in Eq. (4a) can be obtained at a certain value of aspect ratios and material properties of the plate.

Table 1 Boundary conditions at unloaded edges

Boundary at $\eta=0$ or 1	Conditions
Simple (S)	$w=0$ $\frac{\partial^2 w}{\partial \eta^2}+\nu_{xy}s^2\frac{\partial^2 w}{\partial \xi^2}=0$
Fixed (F)	$w=0$ $\frac{\partial w}{\partial \eta}=0$
Free (Fr)	$\frac{\partial^2 w}{\partial \eta^2}+\nu_{xy}s^2\frac{\partial^2 w}{\partial \xi^2}=0$ $\frac{\partial^3 w}{\partial \eta^3}+(2\lambda_2^2-\nu_{xy})s^2\frac{\partial^3 w}{\partial \xi^2 \partial \eta}=0$
Rotationally restrained (R)	$w=0$ $\frac{\partial w}{\partial \eta}-\frac{1}{\varepsilon}\frac{\partial^2 w}{\partial \eta^2}=0 \quad \left(\varepsilon=\frac{\zeta b}{D_y}\right)$

ζ : bending moment per unit rotation per unit length at restrained edge

4. Approximate Solutions

4.1 General solution of energy approach

The principle of conservation of energy which is one of the energy methods can be used to find the buckling coefficient of orthotropic plate with specific loading and boundary conditions [13].

Since the buckling stress is the same throughout the plate when buckling occurs, only one half-sine wave length of plate ($=a/m$) can be considered to find the buckling strength of the plate as shown in Fig. 1.

Assuming the deflection in the transverse direction is a function of η only as a general case, the deflection function can be taken as following Levy's,

$$w=f(\eta)\sin(m\pi\xi) \tag{7}$$

The strain energy and the work done by the external forces during buckling are given by, respectively,

$$\begin{aligned} U=&\frac{ab}{2}\int_0^1\int_0^1\left\{\frac{D_x}{a^4}\left(\frac{\partial^2 w}{\partial \xi^2}\right)^2\right. \\ &+2\frac{\nu_{yx}D_x}{a^2b^2}\left(\frac{\partial^2 w}{\partial \xi^2}\right)\left(\frac{\partial^2 w}{\partial \eta^2}\right) \\ &\left.+\frac{D_y}{b^4}\left(\frac{\partial^2 w}{\partial \eta^2}\right)^2+4\frac{D_{xy}}{a^2b^2}\left(\frac{\partial^2 w}{\partial \xi \partial \eta}\right)^2\right\}d\xi d\eta \end{aligned} \tag{8}$$

$$T=\frac{p_0 b}{2a}\int_0^1\int_0^1(1-c\eta)\left(\frac{\partial w}{\partial \xi}\right)^2 d\xi d\eta \tag{9}$$

Table 2 Characteristic functions

Boundary condition at $\eta=0,1$	Characteristic function
Simple - Simple (SS)	$SS=\begin{vmatrix}\phi_{0,1} & \phi_{0,3}\\ \phi_{2,1} & \phi_{2,3}\end{vmatrix}$
Fixed - Simple (FS)	$FS=\begin{vmatrix}\phi_{0,2} & \phi_{0,3}\\ \phi_{2,2} & \phi_{2,3}\end{vmatrix}$
Fixed - Fixed (FF)	$FF=\begin{vmatrix}\phi_{0,2} & \phi_{0,3}\\ \phi_{1,2} & \phi_{1,3}\end{vmatrix}$
Simple - Free (SFr)	$SFr=\begin{vmatrix}\phi_{2,1}-\chi_m\phi_{0,1} & \phi_{2,3}-\chi_m\phi_{0,3}\\ \phi_{3,1}-(2\lambda_{2m}-\chi_m)\phi_{1,1} & \phi_{3,3}-(2\lambda_{2m}-\chi_m)\phi_{1,3}\end{vmatrix}$
Fixed - Free (FFr)	$FFr=\begin{vmatrix}\phi_{2,2}-\chi_m\phi_{0,2} & \phi_{2,3}-\chi_m\phi_{0,3}\\ \phi_{3,2}-(2\lambda_{2m}-\chi_m)\phi_{1,2} & \phi_{3,3}-(2\lambda_{2m}-\chi_m)\phi_{1,3}\end{vmatrix}$
Restained - Restrained (RR)	$RR=\varepsilon_1\varepsilon_2\cdot FF+\varepsilon_1\cdot FS+2\varepsilon_2\cdot SF+2\cdot SS$
Restrained - Free (RFr)	$RFr=FFr+\frac{2}{\varepsilon_1}SFr$

where, $\phi_{i,j}=\sum_{n=i}^{\infty}\frac{n!}{(n-i)!}B_{n,j}$, $\chi_m=\nu_{xy}m^2\pi^2s^2$

Substituting Eq. (7) into Eqs. (8) and (9), and evaluating the integral in the direction of ξ-axis, the strain energy and the work done are formulated in terms of derivatives of transverse deflection.

Applying the principle of conservation of energy and the definition of bucking coefficient as defined in Eq. (4 a), the buckling coefficient can be expressed as

$$k=\frac{C_1}{\phi_m^2}+C_2\phi_m^2+C_3 \tag{10}$$

In Eq. (10), ϕ_m is the ratio of half-sine wave length and width of plate, and the constants C_1, C_2, and C_3 are as follows:

$$C_1=\sqrt{\frac{E_x}{E_y}}A_1,\quad C_2=\frac{1}{\pi^4}\sqrt{\frac{E_y}{E_x}}A_3 \tag{11 a,b}$$

$$C_3=\frac{1}{\pi^2}\left\{\frac{4(1-\nu_{xy}\nu_{yx})G_{xy}}{\sqrt{E_xE_y}}A_4-2\nu_{yx}\sqrt{\frac{E_x}{E_y}}A_2\right\} \tag{11 c}$$

$$A_1=\frac{\int_0^1\{f(\eta)\}^2d\eta}{\int_0^1(1-c\eta)\{f(\eta)\}^2d\eta},\quad A_2=\frac{\int_0^1 f(\eta)f(\eta)''d\eta}{\int_0^1(1-c\eta)\{f(\eta)\}^2d\eta} \tag{12 a,b}$$

$$A_3=\frac{\int_0^1\{f(\eta)''\}^2d\eta}{\int_0^1(1-c\eta)\{f(\eta)\}^2d\eta},\quad A_4=\frac{\int_0^1\{f(\eta)'\}^2d\eta}{\int_0^1(1-c\eta)\{f(\eta)\}^2d\eta} \tag{12 c,d}$$

Note that the constants C_1, C_2, and C_3 in Eq. (10) are numerical because the A_1, A_2, A_3, and A_4 are numerical in evaluating the integrals.

Bulson (1969) presented the example problems for isotropic material [13], and Yoon, et al. (1995) extended the same problem to orthotropic material [14]. It was shown that the results obtained by Eq. (10) differed by 5 % to 11 % from the closed-form solutions [15].

Eq. (10) can be evaluated easily if the deflection function for the transverse direction has been assumed. But it is limited to use Eq. (10) when c equal to 2.0, which means that the linearly distributed in-plane forces due to pure bending are applied, because the denominator in Eqs. (12) becomes zero. In addition, the accuracy of result depends on the appropriate assumption of deflection function in the transverse direction.

4.2 Approximate solution

In this study, we suggest the approximate solution to find the buckling coefficient of orthtropic plate whose boundary conditions at the unloaded edges are arbitrary including the rotationally restrained boundary condition as shown in Fig. 1.

Reviewing the published documents [13, 14, 15], the simplified form of equation for the buckling of rectangular orthotropic plate can be assumed as the same form of Eq. (10).

The first derivative of k with respect to ϕ_m at the minimum point of the curve must be vanished, which leads to the equation

$$k_{\min}=2\sqrt{C_1C_2}+C_3 \tag{13}$$

occurring when

Table 3 Elastic constants of various composite materials [8]

Material Type	E_x GPa (ksi)	E_y GPa (ksi)	G_{xy} GPa (ksi)	ν_{xy}
Structural Steel	200.00 (29,000)	200.00 (29,000)	76.92 (11,153)	0.30
BFRP (B4/N4405)	204.00 (29,580)	18.48 (2,680)	5.59 (810)	0.23
CFRP (AS/H3501)	138.00 (20,010)	8.97 (1,300)	7.10 (1,030)	0.30
CFRP (IM6/Epoxy)	203.03 (29,440)	11.17 (1,620)	8.41 (1,220)	0.32
CFRP (T300/F934)	148.00 (21,460)	9.66 (1,400)	4.14 (660)	0.30
CFRP (T300/N5208)	181.03 (26,250)	10.28 (1,490)	7.17 (1,040)	0.28
CFRTP (AS4/PEEK)	134.00 (19,430)	8.90 (1,290)	5.10 (740)	0.28
GFRP (E-glass/Epoxy)	38.62 (5,600)	8.28 (1,200)	4.14 (600)	0.33
GFRP (E-glass/Polyester)	33.45 (4,580)	7.03 (1,020)	2.97 (430)	0.35
GFRP (E-glass/Vinylester)	17.24 (2,500)	6.70 (1,000)	2.93 (425)	0.33
KFRP (Kev49/Epoxy)	76.00 (11,020)	5.52 (800)	2.28 (330)	0.34

$$\phi_m = \left(\frac{C_1}{C_2}\right)^{1/4} \tag{14}$$

C_1 can be assumed as Eq. (15a) for the uniform compression ($c = 0.0$) and Eq. (15b) for the linearly varying in-plane forces ($c = 2.0$), respectively. It was shown that those assumption was reasonable in previous work[13, 14, 15].

$$C_1 = \sqrt{\frac{E_x}{E_y}} \tag{15a}$$

$$C_1 = 2\sqrt{\frac{E_x}{E_y}} \tag{15b}$$

Once the value of C_1 is known, C_2 can be found by substituting the exact value ϕ_m and Eqs. (15) into Eq. (14), and then C_3 can be obtained by using Eq. (13) with obtained values of C_1 and C_2.

As shown in Eqs. (11) and (12), C_2 and C_3 are affected by the mechanical properties and boundary conditions at the unloaded edges of plate.

For three different cases, parametric studies were performed with wide range of commonly used composite materials given in Table 3, and the approximate equation of C_2 and C_3 is obtained, respectively, as follows.

RR Case: Restrained-Restrained boundary conditions at unloaded edges and plate subjected to uniform compression

In this case, the unloaded edges of plate ($y = 0$, b) shown in Fig. 1 are both rotationally restrained ($\varepsilon_1 = \varepsilon_2 = \varepsilon$) and uniform compression is applied at the edges $x = 0$, a. Flange of box-shape compression and flexural members may be modeled as this case.

Using the closed-form solution in Table 2, the minimum buckling coefficient $k_{\min}$ and its corresponding $\phi_{m(k_{\min})}$ were found for various composite materials given in Table 3.

The results obtained by the closed-form solution were regenerated by using Eqs. (17) and (18) and were plotted in Figs. 2 and 3.

$$C_{1RR} = \sqrt{\frac{E_x}{E_y}} \tag{16}$$

$$f_{RR}(\varepsilon) = \frac{C_{1RR}}{\phi^4_{k_{\min}}} \cdot \sqrt{\frac{E_x}{E_y}} \tag{17}$$

$$g_{RR}(\varepsilon) = \frac{C_{3RR}}{\nu_{yx}\sqrt{\frac{E_x}{E_y}} + \frac{2(1-\nu_{xy}\nu_{yx})G_{xy}}{\sqrt{E_x E_y}}} \tag{18}$$

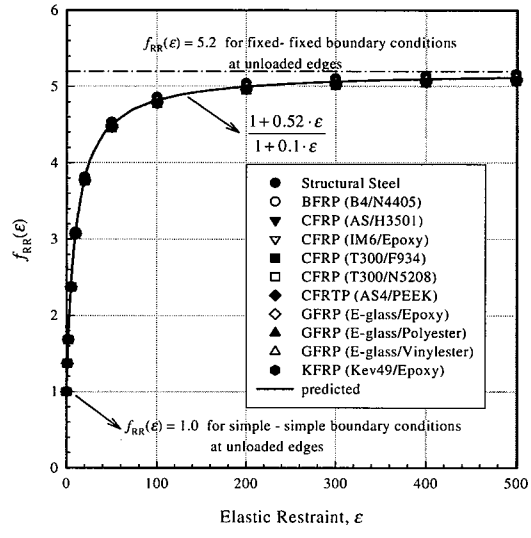

Fig. 2 $f_{RR}(\varepsilon)$ for RR case.

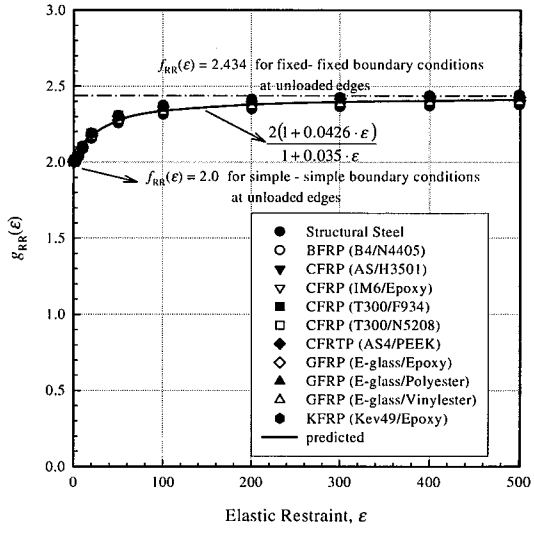

Fig. 3 $g_{RR}(\varepsilon)$ for RR case.

As shown in Figs. 2 and 3, the calculated values of $f_{RR}(\varepsilon)$ and $g_{RR}(\varepsilon)$ are coincided with each other for various composite materials given in Table 3. From the results, C_{2RR} and C_{3RR} can be approximated as

$$C_{2RR} = f_{RR}(\varepsilon)\sqrt{\frac{E_y}{E_x}} \tag{16}$$

$$C_{3RR} = g_{RR}(\varepsilon) \cdot \left\{ \nu_{yx} \sqrt{\frac{E_x}{E_y}} + \frac{2G_{xy}(1-\nu_{xy}\nu_{yx})}{\sqrt{E_x E_y}} \right\} \tag{17}$$

where,

$$f_{RR}(\varepsilon) = \frac{1+0.52\varepsilon}{1+0.1\varepsilon}$$

$$g_{RR}(\varepsilon) = \frac{2(1+0.0426\varepsilon)}{1+0.035\varepsilon}$$

RFr Case: Restrained-Free boundary conditions at unloaded edges and plate subjected to uniform compression

In this case, the unloaded edges of plate ($y=0$, b) shown in Fig. 1 are rotationally restrained ($\varepsilon_1 = \varepsilon$) and free, respectively, and uniform compression is applied at the edges $x=0, a$. The flange of I-shape members may be approximated as this case.

Following the same procedure for the RR case, the results obtained by the closed-form solution were also regenerated by using Eqs. (20) and (21) and were plotted in Figs. 4 and 5.

$$C_{1RFr} = \sqrt{\frac{E_x}{E_y}} \tag{16}$$

$$f_{RFr}(\varepsilon) = \frac{C_{1RFr}}{\phi^4_{k_{min}}} \cdot \sqrt{\frac{E_x}{E_y}} \tag{20}$$

$$g_{RFr}(\varepsilon) = \frac{C_{3RFr}\sqrt{E_x E_y}}{(1-\nu_{xy}\nu_{yx})G_{xy}} \tag{21}$$

As shown in Figs. 4 and 5, the calculated values of $f_{RFr}(\varepsilon)$ and $g_{RFr}(\varepsilon)$ are coincided with each other for various composite materials given in Table 3. From the results, C_{2RFr} and C_{3RFr} can be expressed as Eqs. (22) and (23).

$$C_{2RFr} = f_{RFr}(\varepsilon) \sqrt{\frac{E_y}{E_x}} \tag{22}$$

$$C_{3RFr} = g_{RFr}(\varepsilon) \cdot \frac{G_{xy}(1-\nu_{xy}\nu_{yx})}{\sqrt{E_x E_y}} \tag{23}$$

where,

$$f_{RFr}(\varepsilon) = \frac{0.133\varepsilon}{4.2+\varepsilon}$$

$$g_{RFr}(\varepsilon) = \frac{1+0.156\varepsilon}{0.822+0.097\varepsilon}$$

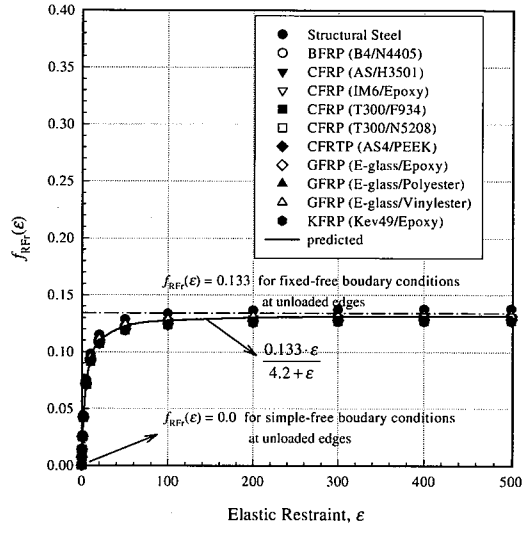

Fig. 4 $f_{RFr}(\varepsilon)$ **for RFr case.**

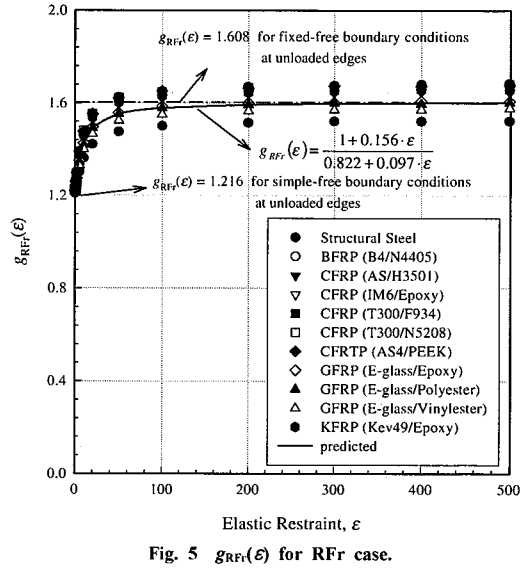

Fig. 5 $g_{RFr}(\varepsilon)$ **for RFr case.**

RS Case: Restrained-Simple boundary conditions at unloaded edges and plate subjected to linearly distributed forces

In this case, the unloaded edges of plate ($y=0$, b) shown in Fig. 1 are rotationally restrained and simple ($\varepsilon_1 = \varepsilon$, $\varepsilon_2 = 0$), respectively, and linearly distributed in-plane forces are applied at edges $x=0$, a. The web of I- and box-shape flexural members may be simplified as this case.

As the same procedure for the RR case, the results obtained by the closed-form solution were regenerated by using Eqs. (25) and (26) and were plotted in Figs. 6 and 7.

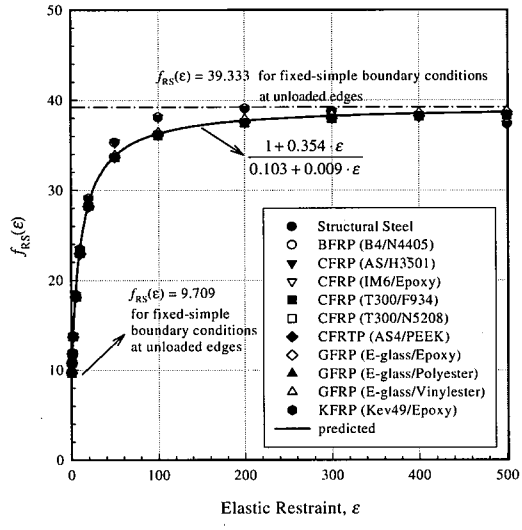

Fig. 6 $f_{RS}(\varepsilon)$ for RS case.

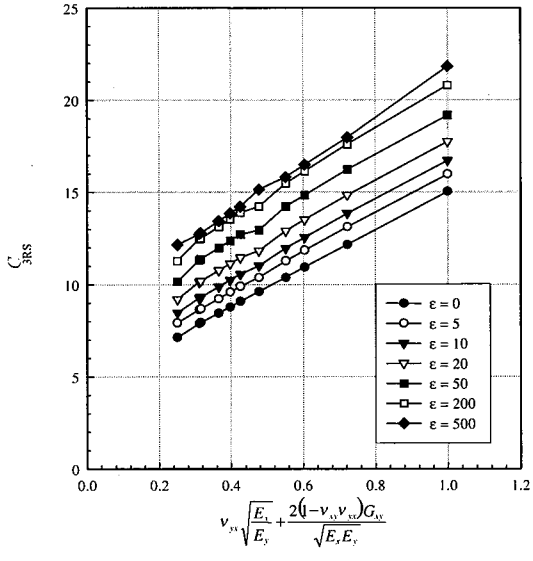

Fig. 7 C_{3RS} for RS case.

$$C_{1RFr}=\sqrt{\frac{E_x}{E_y}} \tag{24}$$

$$f_{RFr}(\varepsilon)=\frac{C_{1RFr}}{\phi^4_{k_{min}}}\cdot\sqrt{\frac{E_x}{E_y}} \tag{25}$$

$$C_{3RS}=k_{min}-2\sqrt{C_{1RS}C_{2RS}} \tag{26}$$

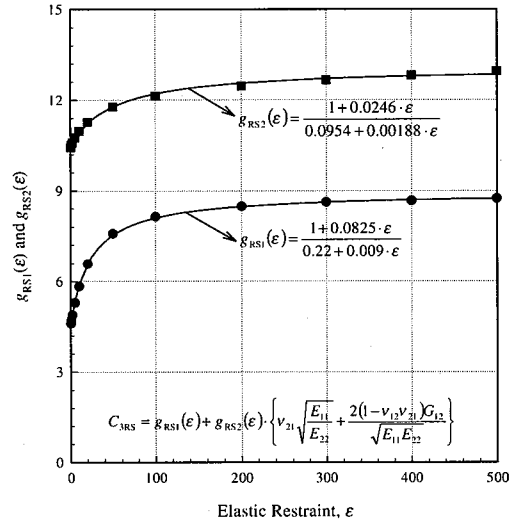

Fig. 8 $g_{RS1}(\varepsilon)$ and $g_{RS2}(\varepsilon)$for RS case.

As shown in Fig. 6, the calculated value of $f_{RS}(\varepsilon)$ is coincided with each other for various composite materials given in Table 3. From the results, C_{2RS} can be expressed as Eq. (27).

$$C_{2RS}=f_{RS}(\varepsilon)\sqrt{\frac{E_y}{E_x}} \tag{27}$$

where,

$$f_{RS}(\varepsilon)=\frac{1+0.354\varepsilon}{0.103+0.009\varepsilon}$$

In Fig. 7, the value of C_{3RS} is varied almost linearly with respect to specific nondimensional value of material properties as shown in horizontal axis, for each elastic restraint.

Therefore, C_{3RS} can be approximated as a linear function,

$$C_{3RS}=g_{RS1}(\varepsilon)+g_{RS2}(\varepsilon)\cdot\left\{\nu_{yx}\sqrt{\frac{E_x}{E_y}}+\frac{2(1-\nu_{xy}\nu_{yx})G_{xy}}{\sqrt{E_xE_y}}\right\} \tag{28}$$

Linear regression was performed for each set of the results with respect to elastic restraint in Fig. 7, $g_{RS1}(\varepsilon)$ and $g_{RS1}(\varepsilon)$ were plotted in Fig. 8, and the approximate equations were

Table 4 Simplified form of equation

RR Case	RFr Case	RS Case
$C_1=\sqrt{\frac{E_x}{E_y}}$ $C_2=f_{RR}(\varepsilon)\sqrt{\frac{E_y}{E_x}}$ $C_3=g_{RR}(\varepsilon)\cdot\left\{\nu_{yx}\sqrt{\frac{E_x}{E_y}}+\frac{2G_{xy}(1-\nu_{xy}\nu_{yx})}{\sqrt{E_xE_y}}\right\}$ $f_{RR}(\varepsilon)=\frac{1+0.52\varepsilon}{1+0.1\varepsilon}$ $g_{RR}(\varepsilon)=\frac{2(1+0.0426\varepsilon)}{1+0.035\varepsilon}$	$C_1=\sqrt{\frac{E_x}{E_y}}$ $C_2=f_{RFr}(\varepsilon)\sqrt{\frac{E_y}{E_x}}$ $C_3=g_{RFr}(\varepsilon)\cdot\frac{G_{xy}(1-\nu_{xy}\nu_{yx})}{\sqrt{E_xE_y}}$ $f_{RFr}(\varepsilon)=\frac{0.133\varepsilon}{4.2+\varepsilon}$ $g_{RFr}(\varepsilon)=\frac{1+0.156\varepsilon}{0.822+0.097\varepsilon}$	$C_1=2\sqrt{\frac{E_x}{E_y}}$ $C_2=f_{RS}(\varepsilon)\sqrt{\frac{E_y}{E_x}}$ $C_3=g_{RS1}(\varepsilon)+g_{RS2}(\varepsilon)\cdot\left\{\nu_{yx}\sqrt{\frac{E_x}{E_y}}+\frac{2(1-\nu_{xy}\nu_{yx})G_{xy}}{\sqrt{E_xE_y}}\right\}$ $f_{RS}(\varepsilon)=\frac{1+0.354\varepsilon}{0.103+0.009\varepsilon}$ $g_{RS1}(\varepsilon)=\frac{1+0.0246\varepsilon}{0.0954+0.00188\varepsilon}$ $g_{RS2}(\varepsilon)=\frac{1+0.0825\varepsilon}{0.22+0.009\varepsilon}$
$k=\frac{C_1}{\phi_m^2}+C_2\phi_m^2+C_3,\quad k_{min}=2\sqrt{C_1C_2}+C_3$		

RR Case : Restrained-Restrained boundary conditions at unloaded edges, plate subjected to uniform compression
RFr Case: Restrained-Free boundary conditions at unloaded edges, plate subjected to uniform compression
RS Case : Restrained-Simple boundary conditions at unloaded edges, plate subjected to linearly distributed in-plane forces

obtained as Eqs. (29) and (30), respectively.

$$g_{RS1}(\varepsilon)=\frac{1+0.0246\varepsilon}{0.0954+0.00188\varepsilon} \tag{29}$$

$$g_{RS2}(\varepsilon)=\frac{1+0.0825\varepsilon}{0.22+0.009\varepsilon} \tag{30}$$

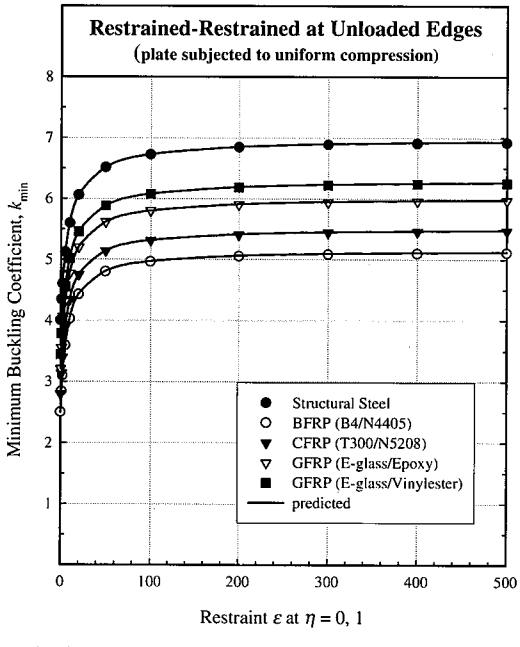

Fig. 9 Minimum buckling coefficient of plate(RR Case).

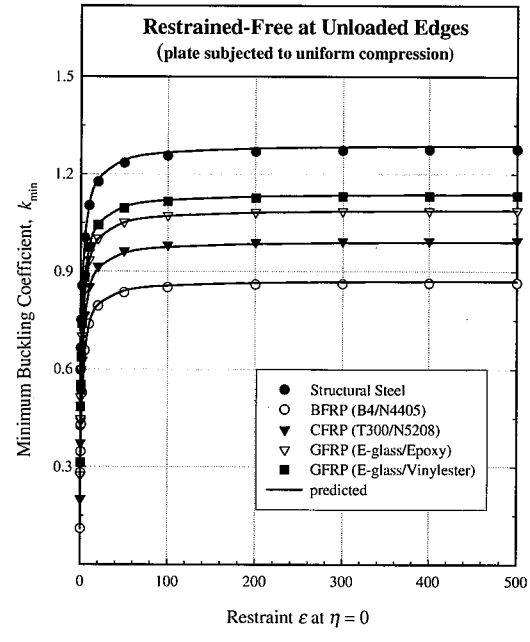

Fig. 10 Minimum buckling coefficient of plate(RFr Case).

Above results are summarized in Table 4, and Figs. 9, 10 and 11 show the results of buckling analysis for the plate with typical orthotropic mechanical properties. In the graphs, the vertical axis indicates the minimum buckling coefficient and the horizontal axis is the elastic restraint. Symbolic values are the results obtained by the closed-form solution

and the solid line is the result obtained by suggested approximate equations in Table 4.

The difference of the results obtained by the approximate solution is less than 1.5%.

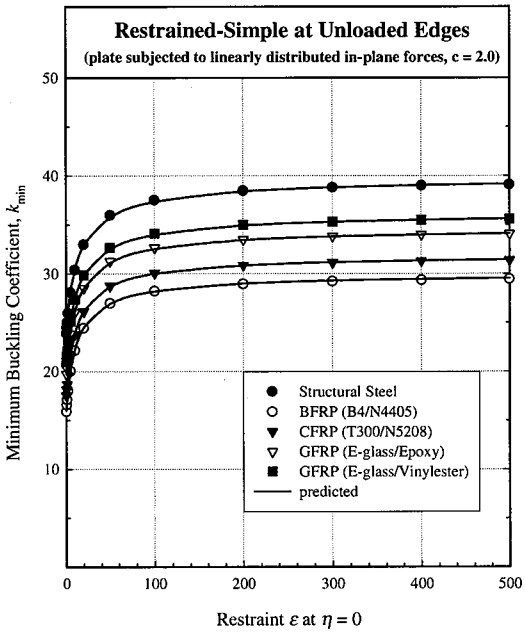

Fig. 11 Minimum buckling coefficient of plate(RS Case).

5. Conclusions

In this paper, we presented the analytical solution for the elastic buckling of orthotropic plate subjected to uniform compression and linearly distributed loads with elastically restrained boundary conditions at unloaded edges. Parametric studies were conducted and the approximate equation was developed to determine the buckling coefficient of orthotropic plate. The results obtained by the simplified form of equation were agreed well with those obtained by the closed-form solution. Therefore, the simplified form of equation proposed in this study can be used effectively to analyze the buckling of orthotropic plate.

In practice, the degree of restraint between plate components of structural members is directly related to the flexural rigidity and ratio of in-plane compressive stress applied on each plate component. Therefore, in order to establish the design criteria relating to the local buckling of orthotropic structural members, further studies need to be conducted to evaluate more appropriate coefficient of restraint for a wide range of FRP structural shapes.

There is also some limit conditions to use those proposed equations for all kind of FRP structural profiles. Since the pultruded shapes were considered in this study, the bending-twisting coupling effect and bending-extension coupling effect were neglected in derivation of differential equation, which can not be negligible in the problem of laminated structural shapes. Therefore, the suggested equations may not be applicable for the buckling problem of general laminated plates.

Acknowledgement

This research was supported by grant No. R01-2002-000-00308-0 from the Basic Research Program of the Korea Science & Engineering Foundation and has been conducted during second author's sabbatical year (3002. 3. 1~ 2004. 2. 29) of Hongik University.

Reference

1) Davalos, J. F., Salim, H. A., Qiao, P., Lopez-Anido, R., and Barbero, E. J., "Analysis and Design of Pultruded FRP Shapes under Bending," *Composites*, Vol. 27B, Elsevier Applied Science Publishers Ltd., England, 1996, pp. 295-305.

2) Wittrick, W. H., "Correlation Between Some Stability Problems for Orthotropic and Isotropic Plates under Bi-Axial and Uni-Axial Direct Stress," *Journal of the Aeronautical Quarterly*, Vol. 4, August, 1952, pp. 83-92.

3) Lekhnitskii, S. G., *Anisotropic Plates*, S. W. Tsai and T. Cheron (Trans.), Gordon and Breach, 2nd printing, New York, 1984.

4) Lee, D. J., "The Local Buckling Coefficient for Orthotropic Stuructural Section," *The Aeronautical Journal*, Vol. 82, No. 811, July, 1978, pp. 313-320.

5) Lee, D. J., "Some Observations on the Local Instability of Orthotropic Structural Sections," *Technical Note, The Aeronautical Journal*, Paper No. 642, March, 1979.

6) Yoon, S. J., "Local Buckling of Pultruded I-Shape Columns," *Ph.D. Thesis*, School of Civil Engineering, Georgia Institute of Technology, Atlanta, Georgia, 1993.

7) Chae, S. H., "A Study on the Analysis of Orthotropic Thin-Walled Short Columns," *Master's Thesis*, Hongik University, Seoul, Korea, 1994.

8) Shih, B. J., "On the Aanalysis of Fiber-Reinforced Polymeric Bridge Components," *Ph.D. Thesis*, School of Civil Engineering, Georgia Institute of Technology, Atlanta, Georgia, 1994.
9) Webber, J. P., Holt, P. J., and Lee, D. A., "Instability of Carbon Fibre Reinforced Flanges of I Section Beams and Columns," *Composite Structures*, Vol. 4, Elsevier Applied Science Publishers Ltd., England, 1985, pp. 245-265.
10) Bank, L. C. and Yin, J., "Buckling of Orthotropic Plates with Free and Rotationally Restrained Unloaded Edges," *Thin-Walled Structures*, Vol. 24, Elsevier Applied Science Publishers Ltd., England, 1996, pp. 83-96.
11) Yoon, S. J. and Jeong, S. K., "Buckling Behavior of Elastically Restrained Orthotropic Plates," *Journal of the Korean Society for Composite Materials*, Vol., 13, No. 3, KSCM, June, 1999, pp. 17-25.
12) Yoon, S. J., Chae, S. H., Jung, J. H., and Kwon, S. M., "Buckling of Elastically Restrained Orthotropic Plate under In-plane Linearly Distributed Uniaxial Load," *Proceedings of the Korean Society of Civil Engineers and Civil Expo* 2001 (CD), Vol. 1, KSCE, November, 2001.
13) Bulson, P. S., *The Stability of Flat Plates*, Americal Elsevier Publishing Company, Inc., New York, 1969.
14) Yoon, S. J., Moon, H. D., and Lee, W. B., "A Study on the Design Criteria Relating to the Local Buckling of Structural Shapes Composed of Orthotropic Thin Plate Elements," *Journal of the Korean Society of Civil Engineers*, KSCE, Vol. 15, No. 3, 1995, pp. 533-544.
15) Yoon, S. J. and Chae, S. H., "Elastic Restraining Effect of Plate Element for Local Buckling of Orthotropic Compression Members," *Journal of the Korean Society of Civil Engineers*, KSCE, Vol. 19, No. I-2, 1999, pp. 203-214.
16) Strongwell, *Extren Fiberglass Structural Shapes Design Manual*, Morrison Molded Fiberglass Company, Bristol, Virginia, 1998.

Appendix

for $0 \leq n \leq 3$

$$B_{n,i} = \begin{cases} 1 & \text{if } n = i \\ 0 & \text{if } n \neq i \end{cases}$$

for $n = 4$

$$B_{n,i} = \alpha_n B_{n-2,i} - (\beta_n - \gamma_n k) B_{n-4,i}$$

for $n \geq 5$

$$B_{n,i} = \alpha_n B_{n-2,i} - (\beta_n - \gamma_n k) B_{n-4,i} - c\gamma_n k B_{n-5,i}$$

where,

$$\alpha_n = \frac{2(n-2)!}{n!}\lambda_{2m}, \quad \beta_n = \frac{(n-4)!}{n!}\lambda_{1m}^2$$

$$\gamma_n = \frac{(n-4)!}{n!}\pi^2\lambda_{1m}, \quad \lambda_{1m} = (\lambda_1 m\pi s)^2$$

$$\lambda_{2m} = (\lambda_2 m\pi s)^2$$